Effect of sintering temperature on crystal structure and physical properties of the $M_{g0,92}Zn_{0,05}C_{0,03}$ Alloy

Budiarto[1]*, Susilo[2]
[1]Program Study of Mechanical Engineering, Faculty Engineering, Jakarta 13630, University Kristen Indonesia
[2]Program Study of Electrical Engineering, Faculty Engineering, Jakarta 13630, Universitas Kristen Indonesia
*Corresponding author: budidamaz@gmail.com

Abstract
The effect of sintering temperature on the crystal structure and physical properties of the $M_{g0,92}Zn_{0,05}C_{0,03}$ alloy has been studied. Magnesium-based alloys are one of the alloys that have been used in industry, the health sector, and as biodegradable materials and biomaterials. The aim of this study was to determine the effect of temperature and sintering holding time on crystal size, dislocation density, microlattice strain, and yield strength. , porosity and density of $M_{g0,92}Zn_{0,05}C_{0,03}$ alloy. $M_{g0,92}Zn_{0,05}C_{0,03}$ alloy was prepared using the powder metallurgy method at sintering temperatures of 475 °C, 525 °C and 575°C with a constant holding time of 90 minutes. The results showed that there was a relationship between sintering temperature as the crystal size and porosity increased, but the dislocation density, micro-strain, yield strength and density decreased inversely for the same length of holding time.

Keywords:
Alloy $M_{g0,92}Zn_{0,05}C_{0,03}$, XRD, crystall size, powder metallurgy

1 Introduction

The development of biomedical materials has contributed significantly to advances in the health sector and the biomedical industry. Porous metals are materials containing porous with a certain volume and with a matrix of metal or non-metal alloys. This material is generally very light due to its low density, but has good performance in terms of mechanical properties [1,2].

Currently, metal foam is also being developed for medical materials in this case implants. The stability of the implant is not only seen from its strength, but also depends on the fixation of the implant to the surrounding tissue. Currently, the fixation of implants can be enhanced by growth of bone tissue through the porous metal matrix, so that the new tissue is directly attached to the underlying bone. Another reason is the nature of metal foam which has a low elastic modulus, so as to avoid shear stress on the bone. The most important thing is to allow body fluids to flow through this porous matrix, so that when bone tissue begins to grow it can form interconnections with other tissues [3,4].

Alloy Magnesium-Calcium-Zinc is a material that is being developed for biomaterial applications because it is biodegradable and resembles bone and the majority are elements needed in the human body. Magnesium naturally occurs in the body and is found in the bones. In blood serum at normal levels

and magnesium in extracellular fluid levels around 0.7-1.06 mmol/l. This Fig. shows that Mg is the second most abundant element in intracellular ions and the fourth most abundant cation in the body. Several studies have shown that Mg ions do not affect tissues when used in the human body [5].

In vitro studies on human osteoblast cells also confirmed that Mg ion does not significantly affect regeneration and viability, besides that Mg metal is non-toxic to the human body. Magnesium is a light metal, with a density of 1.74 g/cm^3, which is much lighter than Al (2.7 gr/cm^3), titanium (4.4-4.5gr/cm^3) and steel (7.75-8.05 g/cm^3) and very close to with the density of bone, which is 1.8-2.1 gr/cm^3. Magnesium is very important in the body's metabolism and is also naturally present in bone tissue [6,7]. C

Ca is a major element that is also present in the body and is important in terms of chemical signaling in cells. In addition, the Mg-Ca alloy has a density similar to that of bone and magnesium is required to incorporate calcium into bones. The maximum solubility of Ca in Mg is about 0.8% at room temperature. The Mg-Ca alloy consists of two phases namely α-Mg and Mg_2Ca, and the presence of this Ca can improve the mechanical properties of the alloy, so that the mechanical properties of this alloy can be determined by controlling the elemental content of Ca [8,9].

Calcium addition up to 4% in pure magnesium will improve its mechanical properties. The higher the concentration at the solubility limit, the formation of the Mg_2Ca intermetallic phase increases the corrosion rate due to the formation of micro-galvanic cells with Mg matrices. The total calcium content in the human body is around 1 kg-1.1 kg, most of it is in bones and teeth and most of it is associated with phosphate and hydroxyapatite in bones [10,11].

The Mg-Zn system is currently receiving great attention because Zn is one of the most abundant nutritional elements in the body and is based safely for biomedical applications. Zn can also improve corrosion resistance and mechanical properties of magnesium alloys [12,13].

In addition, Zn can effectively strengthen magnesium through the solid solution hardening mechanism. According to the Mg-Zn binary phase diagram, the maximum solubility of Zn in Mg is 6.2% at 325°C [14,15].

Based on the research that has been done, the results of in vitro toxicity tests show that Mg-Zn does not poison the body's organs. The Mg-Zn binary alloy has good biocompatibility in the in vivo environment [16].

This is what underlies the development of Mg-Zn-C alloys with the right alloy content and an even mixing process so that the desired phase is formed in the mixing process, so that the desired combination of physical and mechanical properties is obtained. The powder metallurgy method in its manufacture was chosen because it is the easiest to control in terms of pore formation. However, there are some limitations of biomaterials in their current applications, including; - possible release of toxic metal ions through wear and tear or corrosion, - lower biocompatibility leading to tissue loss, and the need for further surgical procedures which increase costs.

The aim of this study was to determine the effect of sintering temperature on crystal structure (crystal size, dislocation density, micro lattice strain) and physical properties (density, porosity and yield strength) of the $M_{g0,92}Zn_{0,05}C_{0,03}$ alloy.

2 Materials and Methods

2.1 Materials

The materials used in this study include Metals Magnesium (Mg), Zink (Zn), Carbon (C), all in powder form and the purity is p.a (pro analysis) from Merck. Equipment : Furnace, hydraulic

press machine, analytical balance, ball mill mixing machine, XRD tool.

2.2 Methods

This study uses the experimental method, while the design used is a one shoot case study. Experiments with this design are to carry out one treatment (treatment) on the workpiece directly observed and recorded or documented the results. The data from the treatment of sintering temperature variations were then tested and the data was entered into the table. From the test results, we then analyzed the data. We got the results from the analysis. We can see the difference in the results of sintering temperature variations on the crystal structure, including crystal size, dislocation density and micro-lattice strain, in addition to density, porosity, and yield strength in $M_{g0,92}Zn_{0,05}C_{0,03}$

2.2.1 Density Test

Density value is a measure of the density of a material. In determining the density of a sample, it can be done by the simplest method, namely the dimensional measurement method. The working procedure for determining the density value (gr/cm³) of a pellet-shaped sample is measuring the diameter and thickness of the sample using a caliper, then weighing the mass of the sample, finding the volume of the sample and calculating the density value using the Eq. 1:

$$\rho = \frac{m}{v} \tag{1}$$

Where is ρ = density of sample (g/cm³), m is massa of sample (g), v is volume of dimention sample (m³).

2.2.2 Porosity

Porosity can be defined as the ratio between the volume of empty holes that are owned by solids (empty volume) with the total volume of solids occupied by solids. Porosity in a material is expressed in (%) the cavity volume fraction of a cavity that is in the material. The amount of porosity in a material varies from 0% to 90% depending on the type and application of the material. The porosity of a material is generally expressed by the following Eq. 2:

$$P = (M_k - M_b)/M_b \times 100\% \tag{2}$$

Where P is Porocity (%), M_k is Mass of dry sample (gram), M_b is Saturation mass grams (grams)

2.2.3 X-Ray Diffractrometer

X-ray diffraction (XRD) is an analytical method used to identify crystalline phases in materials by determining lattice structure parameters and to obtain particle sizes. XRD profiles can also provide qualitative and semi-quantitative data on solids or samples.

Crystallite structure

The x-ray diffractogram pattern is formed from the interaction between the x-ray light beam hitting the sample alloy material $M_{g0,92}Zn_{0,05}C_{0,03}$, if in the test sample the alloy $M_{g0,92}Zn_{0,05}C_{0,03}$. has a sequential structure, then some of the x-ray beams will change direction at an independent angle depending on the structure of the test material for the alloy sample $M_{g0,92}Zn_{0,05}C_{0,03}$ and the wavelength of the x-ray radiation source used. so that it can be determined whether an alloy material $M_{g0,92}Zn_{0,05}C_{0,03}$ has dislocation density, crystal size and micro lattice strain and high yield strength or not.

How to determine an X-ray diffraction angle from the results of testing the alloy material $M_{g0,92}Zn_{0,05}C_{0,03}$, can be determined using the Bragg's law equation as Eq. 3 [19]:

$$n\lambda = 2\ d_{hkl} \sin \theta_{hkl} \tag{3}$$

Where n is Order of diffraction, λ is wavelength of x-rays, d_{hkl} is Distance between diffraction planes with millerhkl index, Θ is Bragg diffraction angle for the diffraction plane

To determine and analyze the size/diameter of crystallites referring to the X-ray diffraction peaks from the diffractogram pattern, the Debye Scherrer equation approach is Eq. 4 [17,19]:

$$D = K\lambda/(\beta \cos\theta) \tag{4}$$

Meanwhile, to determine the microstrain value, the Eq.5 is used:

$$\varepsilon = \beta/((4 \tan\theta)) \tag{5}$$

To determine the value of the dislocation density, the Eq. 6 is used:

$$\rho = 1/D^2 \tag{6}$$

Where is D is Crystal size (nm), P is Dislocation Density, ε is Lattice Strain, K is Form factor of a crystal (0.9-1), Λ is X-ray wavelength (1.54056 Å), β is Value of Full Width at Half Maximum (FWHM) (rad), θ is Diffraction angle (degrees).

After knowing the dislocation density, the yield strength (YS) can be calculated using the Eq. 7 [18,19] :

$$YS = 274,54 + 4,96 \times 10^{-6} \text{ MPa.} \tag{7}$$

3 Results and discussion

3.1 Test results with XRD on alloys $M_{g0,92}Zn_{0,05}C_{0,03}$
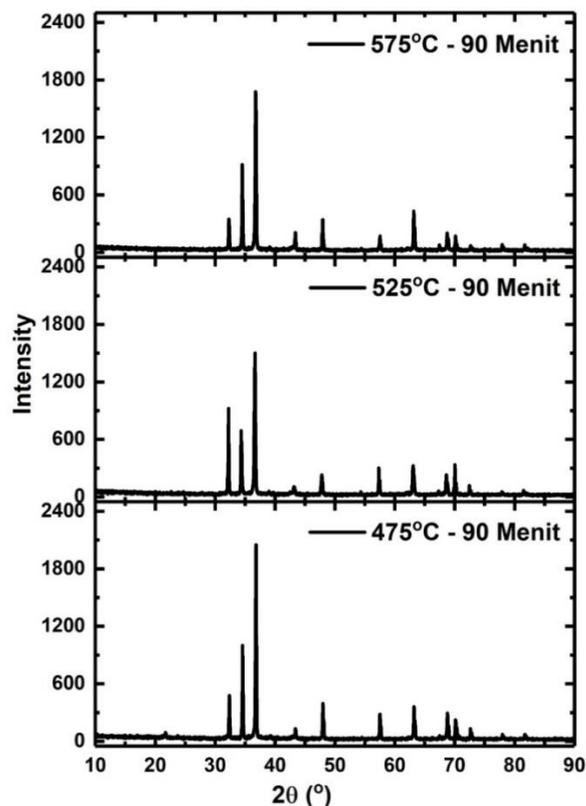
Fig.1. X-ray diffractogram of $M_{g0,92}Zn_{0,05}C_{0,03}$ alloy with temperature variations of 475^0C, 525^0C and 575^0C and sintering time of 90 minutes

Fig. 1 shown that the comparison of the XRD results for the temperature variable can be explained that, for the $Mg_{0,92}Zn_{0,05}C_{0,03}$ alloy, there are 2 phases that appear in this alloy. The first formed phase is α-Mg which is generally the main constituent phase and the second MgZn phase. Previous researchers said that the amount of the second phase (MgZn) present in the Mg matrix is closely related to the corrosion resistance of the Mg alloy. The second phase present in the Mg alloy increases the corrosion rate due to the formation of a galvanic pair between α-Mg and the second phase. The microstructure, mechanics, and corrosion behavior of MgxZn alloy (x = 0.1, 5, 7 wt.%) were investigated to understand the effect of adding different concentrations of Zn in the Mg matrix. The grain size decreases with the addition of Zn. The amount of the second phase (MgZn) in the Mg-Zn alloy increases with increasing Zn content. This situation can be explained based on the Mg – Zn phase diagram, when the Zn content (smaller than 6.2% wt) tends to be in the Mg matrix, and no MgZn phase is formed when it is still within the solubility limit [23].

3.2 Effect of Sintering Temperature on crystal size in alloy $Mg_{0,92}Zn_{0,05}C_{0,03}$

Testing the crystal structure of the alloy $Mg_{0,92}Zn_{0,05}C_{0,03}$ as a result of the sintering process at a temperature of 475 °C and a holding time of 90 minutes with an X-ray diffractometer at an angle of 2θ =10 – 90⁰, a scan speed of 5⁰/minute was performed to determine the crystal size (nm), dislocation density (lines/mm²), and micro-lattice strain. The calculation results from the XRD data are angles 2θ = 20 – 90⁰ and FWHM (β) and included in equations 3, 4, 5, and 6 above, the values for crystal size, dislocation density, and micro lattice strain will be obtained as shown in table 1 and figure 2,3,4.

Table 1. Data of XRD test results for $Mg_{0,92}Zn_{0,05}C_{0,03}$ alloy sintering at 475⁰C and 90 minutes.

No.	Pos. (2θ)	FWHM β (rad)	Crystall Size (nm)	Dislocation Density (line/mm²)	Strain Micro Lattice
1	29,825	0,189	77,66	0,178	0,017
2	32,474	0,157	93,20	0,134	0,012
3	34,797	0,159	91,26	0,128	0,012
4	36,808	0,160	92,18	0,120	0,012
5	43,619	0,179	83,88	0,112	0,014
6	47,971	0,236	64,55	0,132	0,024
7	57,767	0,206	77,99	0,093	0,016
8	63,452	0,189	87,78	0,075	0,013
9	68,912	0,209	81,11	0,076	0,015
10	70,304	0,229	74,55	0,081	0,018

Testing the crystal structure of the alloy $Mg_{0,92}Zn_{0,05}C_{0,03}$ as a result of the sintering process at a temperature of 525 °C and a holding time of 90 minutes with an X-ray diffractometer at an angle of 2θ =10 – 90⁰, a scan speed of 5⁰/minute was performed to determine the crystal size (nm), dislocation density (lines/mm²), and micro-lattice strain. The calculation results from the XRD data are angles 2θ = 20 – 90⁰ and FWHM (β) and included in equations 3, 4, 5, and 6 above, the values for crystal size, dislocation density, and micro lattice strain will be obtained as shown in table 2 and figure 2,3,4.

Testing the crystal structure of the alloy $Mg_{0,92}Zn_{0,05}C_{0,03}$ as a result of the sintering process at a temperature of 575 °C and a holding time of 90 minutes with an X-ray diffractometer at an angle of 2θ =10 – 90⁰, a scan speed of 5⁰/minute was performed to determine the crystal size (nm), dislocation density (lines/mm²), and micro-lattice strain. The calculation results from the XRD data are angles 2θ = 20 – 90⁰ and FWHM (β) and included in equations 3, 4, 5, and 6 above, the values for crystal

size, dislocation density, and micro lattice strain will be obtained as shown in table 3 and figure 2,3,4.

Table 2. Data of XRD test results for $Mg_{0,92}Zn_{0,05}C_{0,03}$ alloy sintering at 525⁰C and 90 minutes.

No.	Pos. (2θ)	FWHM β (rad)	Crystall Size (nm)	Dislocation Density (line/mm²)	Strain Micro Lattice
1	29,92	0,187	76,33	0,178	0,017
2	32,74	0,155	93,43	0,134	0,012
3	34,97	0,158	91,21	0,128	0,012
4	36,77	0,159	91,24	0,120	0,012
5	43,44	0,178	83,43	0,112	0,014
6	47,87	0,234	64,98	0,132	0,024
7	57,88	0,203	77,66	0,093	0,016
8	63,33	0,185	87,62	0,075	0,013
9	68,76	0,208	81,11	0,076	0,015
10	70,22	0,228	75,22	0,081	0,018

Table 3. Data of XRD test results for $Mg_{0,92}Zn_{0,05}C_{0,03}$ alloy sintering at 575⁰C and 90 minutes.

No.	Pos. (2θ)	FWHM β (rad)	Crystall Size (nm)	Dislocation Density (line/mm²)	Strain Micro Lattice
1	29,43	0,163	87,94	0,155	0,013
2	32,13	0,137	11,10	0,113	0,008
3	34,34	0,115	12,62	0,093	0,006
4	36,75	0,128	12,17	0,091	0,007
5	43,21	0,149	10,02	0,094	0,010
6	47,85	0,142	10,67	0,080	0,009
7	57,37	0,152	10,39	0,070	0,009
8	63,14	0,135	12,04	0,055	0,007
9	68,57	0,153	10,97	0,056	0,008
10	69,98	0,172	9,954	0,061	0,010
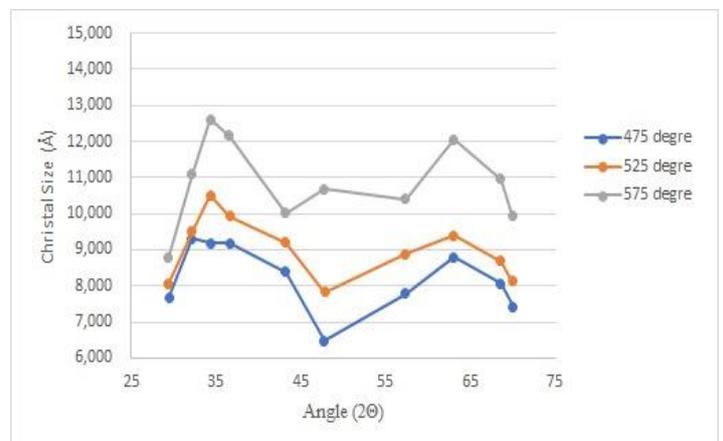
Fig. 2. Effect of sintering temperature and angle 2θ on the crystal size of the alloy $Mg_{0,92}Zn_{0,05}C_{0,03}$

Fig. 2, shows a graph of the effect of sintering temperature of 475°C and a holding time of 90 minutes produces several X-ray diffraction peaks on crystal size which is calculated by the Derby Scherrer equation, where the higher the sintering temperature and the fixed time of 90 minutes indicates that the average crystal size increases. Most of this is due to the process of recrystallization and grain growth during sintering. According to previous researchers [23] said that research on the effect of Zn on the microstructure, mechanical properties and corrosion properties of Mg – Zn alloys. From the microstructural results, it can be seen that the Mg – Zn alloy generally still contains α – Mg matrices and second phases which are distributed along the grain boundary. Also, an increase in zinc content in the alloy will lead to a decrease in grain size.

3.3 Effect of Sintering Temperature on Dislocation Density in alloy $Mg_{0,92}Zn_{0,05}C_{0,03}$
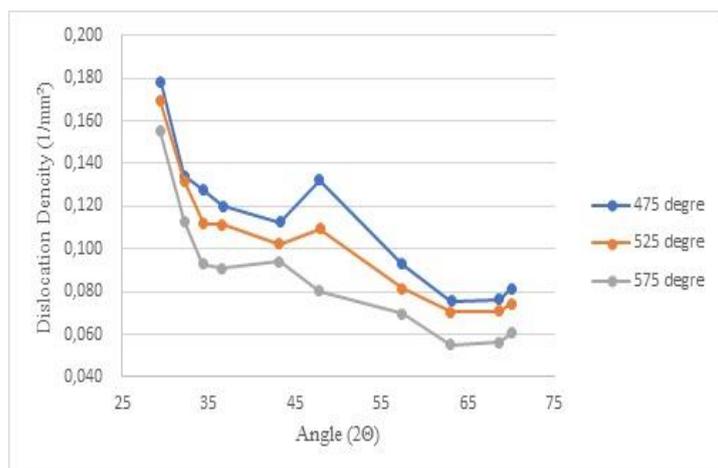
Fig. 3. Effect of sintering temperature and angle 2θ on the dislocation density of the alloy $Mg_{0,92}Zn_{0,05}C_{0,03}$

Fig. 3 shows a graph of the relationship between sintering temperature and angle 2θ to dislocation density and 90 minutes holding time of $Mg_{0,92}Zn_{0,05}C_{0,03}$ alloy, showing that the dislocation density value decreases with increasing sintering temperature. The results of the dislocation density test show that the greater the sintering temperature the lower the dislocation density.

3.4 Effect of Sintering Temperature on Micro Lattice Strain in alloy $Mg_{0,92}Zn_{0,05}C_{0,03}$

Fig. 4 shows a graph of the relationship between sintering temperature and angle 2θ to micro-lattice strain and holding time of 90 minutes for $Mg_{0,92}Zn_{0,05}C_{0,0}$ alloy, showing that the microstrain value gets smaller with increasing sintering temperature.
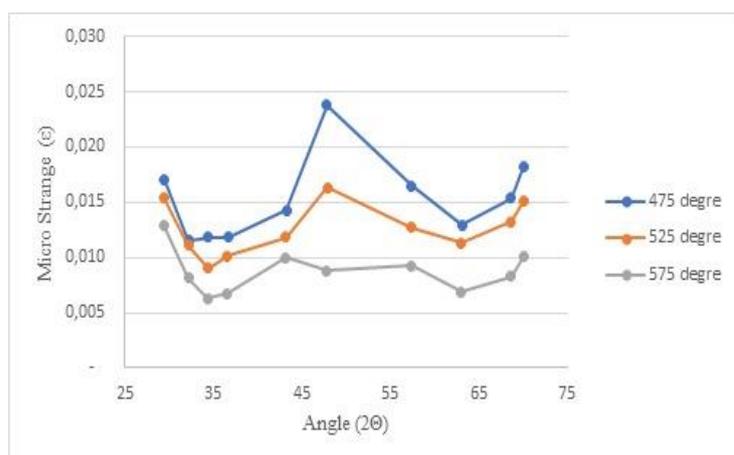
Fig. 4. Effect of sintering temperature and angle 2θ on the micro lattice strain of the alloy $Mg_{0,92}Zn_{0,05}C_{0,03}$

These results are closely related to the reduction in line shape crystal defects (dislocations). Due to an increase in the line shape crystal defects indicated by an increase in the value of the micro lattice strain which results in an increase in the dislocation density. Because the lattice microstrain affects the length of the dislocation lines per unit volume of crystal.

3.4 Effect of sintering temperature on the yield strengt of the alloy $Mg_{0,92}Zn_{0,05}C_{0,03}$
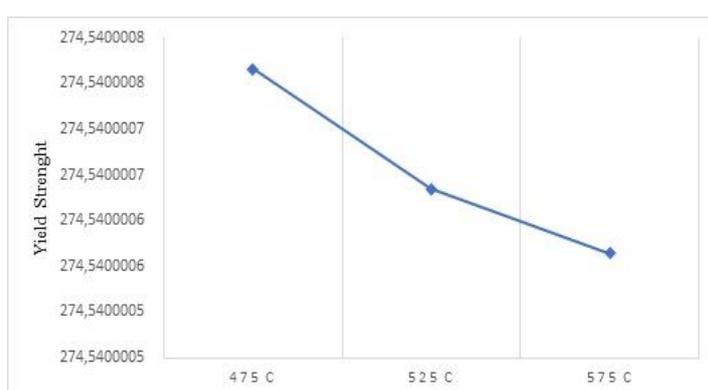
Fig. 5. Effect of sintering temperature on the yield strengt of the alloy $Mg_{0,92}Zn_{0,05}C_{0,03}$

Fig. 5 shows the yield strength values of $Mg_{0,92}Zn_{0,05}Ca_{0,03}$ alloy resulting from sintering temperature variations of 475^0C, 525^0C, and $575\ ^0C$ and holding time for 90 minutes, namely 274. 5400008 MPa, 274.5400007 MPa, and 274.540006 MPa . This indicates that the decrease in yield strength may be due to the recrystallization process and grain growth during the sintering process. As explained in the crystallite size explanation, the majority of plastic deformation of MgZnC alloy occurs through slip and twin dislocation processes. Thus the stress loads imposed on the material do not turn into grain strain but become rotations in the crystal lattice. This shift of the crystal lattice produces crystallites. With increasing calcination time, the dislocation density decreases and consequently the yield strength decreases, this is due to the melting point of Zn 419.58 ^0C. This has been done by previous studies with a porosity of 30-90% [20].

3.5 Effect of sintering temperature on the porocity of the alloy $Mg_{0,92}Zn_{0,05}C_{0,03}$
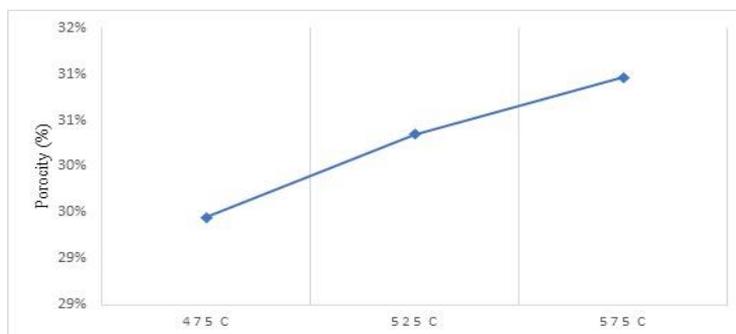
Fig.6. Effect of sintering temperature on the porocity of the alloy $Mg_{0,92}Zn_{0,05}C_{0,03}$

Fig. 6 shows that the porosity value with longer sintering time tends to increase. This happens because it follows the pattern of sintering process phenomena. In addition, this may be due to the enlargement of the grains during the sintering process. Therefore using the powder metallurgy method will produce a material shaft that is easy to control in each alloy sample when compared to the method of making bone implants by casting. It is hoped that the powder metallurgy method is suitable for the manufacture of biomaterial bone implants because the porous structure of magnesium will lead to faster cell growth. By doing a comparison of previous research where the porosity value is 30-90% [20]. The results of previous studies with SEM-EDXS have also been strengthened. It can be seen that the pores formed with larger sizes occur at a sintering temperature of 600 °C. This

indicates that an increase in sintering temperature results in shrinkage of the pores between the grain boundaries (grain boundaries) and is followed by grain growth and increased bonding between adjacent particles [17,21].

3.6 Effect of sintering temperature on the density of the alloy $Mg_{0,92}Zn_{0,05}C_{0,03}$
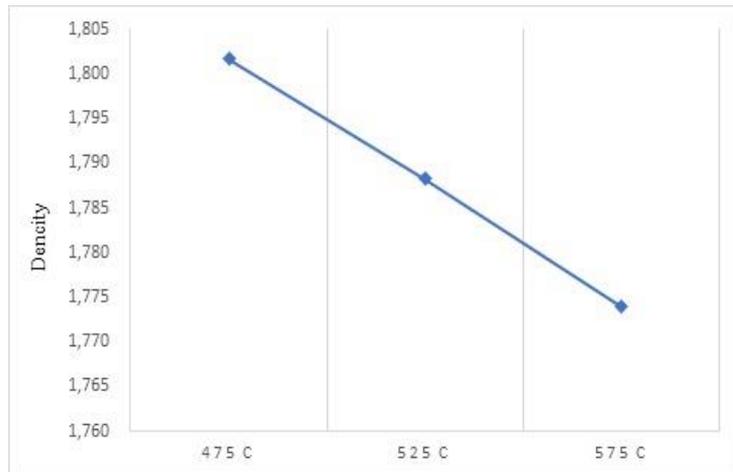
Fig.7. Effect of sintering temperature on the density of the alloy $Mg_{0,92}Zn_{0,05}C_{0,03}$

Fig.7 shows a graph of the relationship between the density values of various sintering temperatures and a fixed time of 90 minutes for the $Mg_{0,92}Zn_{0,05}C_{0,03}$ alloy. Where this graph shows that the density value increases with increasing sintering temperature, this is due to the recrystallization process and grain growth in the $Mg_{0,92}Zn_{0,05}C_{0,03}$ alloy. Where during the sintering process, the greater the temperature the object or material tends to be denser. However, when compared with the cortical bone density value, which is 1.81 ~ 2.0 gr/cm3, it is almost appropriate at this 90 minute time [20]. Please note that with increasing heating temperature, the reaction that occurs is higher. This causes the grain boundaries to start moving so that the grains start to grow, forming channels that are interconnected so that the bond intensity between the elements is higher which makes the alloy tighter. The bond speed is affected by temperature as the driving energy which causes diffusion between grain boundaries and shrinkage of porosity which will increase density and increase strength. In addition, the formation of micropores is also caused by the evaporation of Zn due to the influence of temperature. At sintering temperatures of 600°C and 650 °C the temperature is too high for Zn, thus forming micro pores in the alloy Mg-Ca-Zn [22,24].

4 Conclusion

Based on the test results and analysis of the alloy $Mg_{0,92}Zn_{0,05}C_{0,03}$, it can be concluded as follows: From the results of the crystal structure test with XRD it was shown that the α-Mg phase was formed as the parent phase and the MgZn phase and the sintering temperature was greater and the holding time remained 90 minutes resulting in the crystal size increases, but the micro lattice strain values, dislocation densities, and yield strength decrease. Also for the porosity value and density value, the opposite is true, that is, the higher the sintering temperature, the greater the porosity, but the smaller the density value. The results of the study showed that the $Mg_{0,92}Zn_{0,05}C_{0,03}$ alloy with a compaction pressure of 10 tons has the opportunity to become an implantable biomaterial which has a density value of around 1.800 gram/cm^3 and a yield strength of around 274 MPa.

References

[1] R. Radha and D. Sreekanth, "Insight of magnesium alloys and composites for orthopedic implant applications – a review," *Journal of Magnesium and Alloys*, vol. 5, no. 3, pp. 286–312, Sep. 2017, doi: 10.1016/j.jma.2017.08.003.

[2] S. Agarwal, J. F. Curtin, B. Duffy, and S. Jaiswal, "Biodegradable magnesium alloys for orthopaedic applications: A review on corrosion, biocompatibility and surface modifications," *Materials Science and Engineering: C*, vol. 68, pp. 948–963, Nov. 2016, doi: 10.1016/j.msec.2016.06.020.

[3] B. Zhang, Y. Wang, and L. Geng, "Research on Mg-Zn-Ca Alloy as Degradable Biomaterial," in *InTech eBooks*, 2011. doi: 10.5772/23929.

[4] Y. H. Zheng, X. Gu, and F. Witte, "Biodegradable metals," *Materials Science and Engineering R*, vol. 77, pp. 1–34, Mar. 2014, doi: 10.1016/j.mser.2014.01.001.

[5] Y. Xin, K. Huo, H. Tao, G. Tang, and P. K. Chu, "Influence of aggressive ions on the degradation behavior of biomedical magnesium alloy in physiological environment," *Acta Biomaterialia*, vol. 4, no. 6, pp. 2008–2015, Nov. 2008, doi: 10.1016/j.actbio.2008.05.014.

[6] Z. S. Seyedraoufi and Sh. Mirdamadi, "Synthesis, microstructure and mechanical properties of porous Mg☐Zn scaffolds," *Journal of the Mechanical Behavior of Biomedical Materials*, vol. 21, pp. 1–8, May 2013, doi: 10.1016/j.jmbbm.2013.01.023.

[7] D. Yang *et al.*, "Fabrication of cellular Mg alloy by gas release reaction via powder metallurgical approach," *Metal Powder Report*, vol. 72, no. 2, pp. 124–127, Mar. 2017, doi: 10.1016/j.mprp.2016.02.053.

[8] N. Sezer, Z. Evis, S. M. Kayhan, A. Tahmasebifar, and M. Koç, "Review of magnesium-based biomaterials and their applications," *Journal of Magnesium and Alloys*, vol. 6, no. 1, pp. 23–43, Mar. 2018, doi: 10.1016/j.jma.2018.02.003.

[9] N. V. Pulagara, S. Saini, and R. S. Dondapati, "A Study of Manufacturing and Mechanical Properties of Mg-foam Using Dolomite as the Blowing Agent: A Review," *Progresses in Nanotechnology and Nanomaterials*, vol. 4, no. 1, pp. 7–10, Jan. 2015, doi: 10.5963/pnn0401002.

[10] S. Sánchez, E. Pellicer, S. Suriñach, M. D. Baró, and J. Sort, "Biodegradation and Mechanical Integrity of Magnesium and Magnesium Alloys Suitable for Implants," in *InTech eBooks*, 2013. doi: 10.5772/55584.

[11] A. B. Kennedy, "Porous Metals and Metal Foams Made from Powders," in *InTech eBooks*, 2012. doi: 10.5772/33060.

[12] A. Erryani, F. Pramuji, D. Annur, M. I. Amal, and I. Kartika, "Microstructures and Mechanical Study of Mg Alloy Foam Based on Mg-Zn-Ca-CaCO$_3$ System," *IOP Conference Series*, vol. 202, p. 012028, May 2017, doi: 10.1088/1757-899x/202/1/012028.

[13] I. Kartika, A. R. Ashari, A. Trenggono, F. P. Lestari, and A. Erryani, "Analisis Struktur Pori dan Sifat Mekanik Paduan Mg-0,5Ca-4Zn Hasil Proses Metalurgi Serbuk dengan Variasi Komposisi Foaming Agent CaCO3 dan Temperatur Sintering," *TEKNIK*, vol. 40, no. 3, p. 142, Dec. 2019, doi: 10.14710/teknik.v40i3.25327.

[14] Y. Li, P. Hodgson, and C. Wen, "The effects of calcium and yttrium additions on the microstructure, mechanical properties and biocompatibility of biodegradable magnesium alloys," *Journal of Materials Science*, vol. 46, no. 2, pp. 365–371, Sep. 2010, doi: 10.1007/s10853-010-4843-3.

[15] P. Syafri and I. Isranuri, "Studi Pengaruh Magnesium terhadap Kekuatan Impak dan Mikrostruktur Alumunium Foam Menggunakan 3% CaCO sebagai Blowing Agent', *Jurnal eDinamis*, vol. 5, no. 1, pp. 23–28, 2013.

[16] A. H. M. Yusop, A. A. Bakir, N. A. Shaharom, M. R. A. Kadir, and H. Hermawan, "Porous biodegradable metals for hard tissue scaffolds: a review.," *International Journal of Biomaterials*, Jan. 2012, doi: 10.1155/2012/641430.

[17] F. P. Lestari, B. A. Saputra, A. Erryani, I. Mulyati, M. S. Dwijaya, and I. Kartika, "Analisis Variasi Temperatur Sintering dan Ukuran Agen Pengembang Dolomit terhadap Fabrikasi Paduan Logam Mg-Ca-Zn Berpori Tertutup dengan Proses Metalurgi Serbuk," *TEKNIK*, vol. 42, no. 2, pp. 128–136, Aug. 2021, doi: 10.14710/teknik.v42i2.36978.

[18] F. Sugondo, "Pengaruh Deformasi Pada Karakteristik Kristalit Dan Kekuatan Luluh Zircaloy-4", PTEBN, BATAN Serpong. 2007.

[19] E. B. Sihite and B. Budiarto, "Analisis Pengaruh Pemanasan Penuaan dan Media Pendingin Terhadap Kekerasan, Struktur Mikro dan Struktur Kristal Paduan CuHfCo," *Jurnal Kajian Ilmiah*, vol. 19, no. 3, pp. 231–238, Sep. 2019, doi: 10.31599/jki.v19i3.462.

[20] I. B. Kurniawan, 'Pengaruh Penambahan Zn dan Tekanan Kompaksi Tergadap, Struktur Mikro, Sifat Mekanik dan Laju Peluruhan Paduan Mg-Zn Untuk Aplikasi Orthopedic Devices Dengan Metode Metallurgy Serbuk"', *Jurusan Teknik Material dan Metalurgi*, 2017.

[21] A. Hermanto, Y. Burhanudin, and I. Sukmana, "Peluang dan tantangan aplikasi baut tulang mampu terdegradasi berbasis logam magnesium," *Dinamika Teknik Mesin*, vol. 6, no. 2, Dec. 2016, doi: 10.29303/d.v6i2.11.

[22] H. Nurrohman, 'Pengaruh Variasi Temperatur Dan Waktu Holding Sintering Terhadap Sifat Mekanik Dan Morfologi Biodegradable Material Mg-Fe-Zn Dengan Metode Metalurgi Serbuk Untuk Aplikasi Orthopedic Devices', International Journal of Hypertension, no. 1, 2017.

[23] S. Cai, T. Lei, N. Li, and F. Feng, "Effects of Zn on microstructure, mechanical properties and corrosion behavior of Mg–Zn alloys," *Materials Science and Engineering: C*, vol. 32, no. 8, pp. 2570–2577, Dec. 2012, doi: 10.1016/j.msec.2012.07.042.

[24] Y. Zhou, A. Jiang, and J. Liu, "The Effect of Sintering Temperature to the Microstructure and Properties of AZ91 Magnesium Alloy by Powder Metallurgy," *Applied Mechanics and Materials*, vol. 377, pp. 250–254, Aug. 2013, doi: 10.4028/www.scientific.net/amm.377.250.

[25] L. Yang *et al.*, "Microstructures and mechanical properties of AZ31 magnesium alloys fabricated via vacuum hot-press sintering," *Journal of Alloys and Compounds*, vol. 870, p. 159473, Jul. 2021, doi: 10.1016/j.jallcom.2021.159473.